Crystal Structure of Poly(1,5-naphthalenebenzobisthiazole)

Soo-Young Park,*,† Sang-Cheol Moon,† Thuy D. Dang,‡ N. Venkatasubramanian,§ Jar-wha Lee,⊥ and B. L. Farmer‡

Department of Polymer Science, Kyungpook National University, #1370 Sankyuk-dong, Buk-gu, Daegu 702-701, Korea; AFRL/MLBP, Materials & Manufacturing Technology Directorate, Wright-Patterson Air Force Base, 2941, Hobson Way, Suite 1, Dayton, Ohio 45433-7750; University of Dayton Research Institute, 300 College Park Drive, Dayton, Ohio 45469; and Syscom Technology Inc., 4180 Anson Drive, Hilliard, Ohio 43026

Received October 3, 2004; Revised Manuscript Received December 10, 2004

ABSTRACT: The rigid-rod polymer poly(1,5-naphthalenebenzobisthiazole) (Naph-1,5-PBT) was synthesized and spun into fibers from the lyotropic mesophase of the polymer in polyphosphoric acid by a dry-jet wet spinning method. The crystal structure of naph-1,5-PBT fibers was investigated using X-ray diffraction and molecular modeling methods. The 19 reflections, resolved from the X-ray pattern of the annealed Naph-1,5-PBT fiber, indicate that Naph-1,5-PBT has a perfect crystal structure without axial disorder, unlike other rigid-rod polymers such as poly(*p*-phenylenebenzobisthiazole) (PBT) and poly(*p*-phenylenebenzobisoxazole) (PBO). The observed reflections can be indexed with the triclinic unit cell parameters of $a = 7.31$ Å, $b = 3.68$ Å, $c = 12.68$ Å, and $\beta = 115.1°$ with the space group of $P\bar{1}$, which one monomeric unit is. The torsion angle $\phi = 138°$, at which the naphthalene unit is rotated toward the heterocyclic nitrogen atom, is derived from ab initio energy calculations as well as from the LALS refinement. The LALS refinement shows that the naphthalene ring is rotated by $4.4 \pm 4.6°$ from the *ac* plane on the projection along the *c* axis, and the chains are staggered side-by-side by *c*/4 in a regular way in the *ac* plane. The kinked structure, arising due to the naphthalene unit, as well as the twist structure introduced by the steric interaction between the naphthalene and heterocyclic rings, prevents axial disorders in the crystal which are usually observed in the rigid-rod polymers.

Introduction

Rigid-rod polymers such as poly(*p*-phenylenebenzobisthiazole) (PBT) and poly(*p*-phenylenebenzobisoxazole) (PBO) have attracted attention because of their excellent thermal and thermoxidative stability as well as their exceptional tensile strength and tensile modulus, attributable to their inherent chain stiffness and a high degree of molecular orientation, which is achieved by fiber-spinning from a liquid crystalline solution.[1−18] PBT and PBO fibers have been considered as alternatives to reinforcement aramid and carbon fibers. The crystal structures of PBO and PBT have been investigated by several groups.[19−23] One of the prominent structural characteristics is the axial disorder in the crystal, which causes streaks along the layer lines in the X-ray fiber pattern. Fratini et al.[19] first reported the crystal structure of PBT in which two molecular chains pass through a monoclinic unit cell with unit cell parameters of $a = 11.79$ Å, $b = 3.54$ Å, $c = 12.51$ Å, and $\gamma = 94.0°$, and the plane group of *P*2; the plane group rather than the space group can be considered as being the cause of the axial disorder. They adopted nonprimitive cells in order to include longitudinal and lateral disorders because primitive cells require perfect registry of the adjacent chains, and close intermolecular contact occurs between neighboring molecules along the *a* axis. Takahashi et al.[22−24] recently reported an oblique unit cell with parameters $a = 11.60$ Å, $b = 3.588$ Å, $c = 12.51$ Å, and $\gamma = 92.0°$, and the plane group of *P*2. In the disordered structure, the molecular heights were disordered by $^1/_2$ of the repeat distance on the *ac* plane and by every $^1/_5$ of the repeat distance on the *bc* plane. The torsion angle between the benzobisthiazole and phenyl rings arises from the steric interaction between the *ortho* hydrogen of the phenyl group and the sulfur of the heterocyclic ring. Fratini et al.[19] reported a torsion angle of 46°, which was determined from the X-ray fiber pattern. A single crystal from a model compound for PBT, however, showed a torsion angle of 23°.[16] Takahashi et al.[22−24] also reported a torsion angle of 20.5°, which was close to the calculated values of 27°,[25,26] 20°,[14] 21°,[27] and 29°.[28]

In this study, the structure of Naph-1,5-PBT was delineated using X-ray and molecular modeling methods. Lower geometrical symmetry and extended planar packing of the naphthalene-1,5-diyl structural link relative to the *p*-phenylene unit can affect chain conformation, packing, and crystallinity in analogy to PEN versus PET fibers.[29] The shape of the chain in the Naph-1,5-PBT is kinked compared to PBT due to the 1,5 positions at which the naphthalene ring extends. The kinked structure can distinguish the crystal structure of Naph-1,5-PBT from that of PBT in terms of the axial disorder because of the difficulty in the occurrence of the axial shift. Its crystal structure analysis would be interesting from the structural point of view, since the kinked structure can reduce the axial shift and increase interchain interactions.

Experimental Section

Materials. 2,5-Diamino-1,4-benzenedithioldihydrochloride (DABDT) was obtained through custom synthesis by known preparative routes. It was further purified by recrystallization

† Kyungpook National University.
‡ Wright-Patterson Air Force Base.
§ University of Dayton Research Institute.
⊥ Syscom Technology Inc.
* To whom correspondence should be addressed: Tel +82-53-950-5630; Fax +82-53-950-6623; e-mail psy@knu.ac.kr.

10.1021/ma047967y CCC: $30.25
Published on Web 02/05/2005

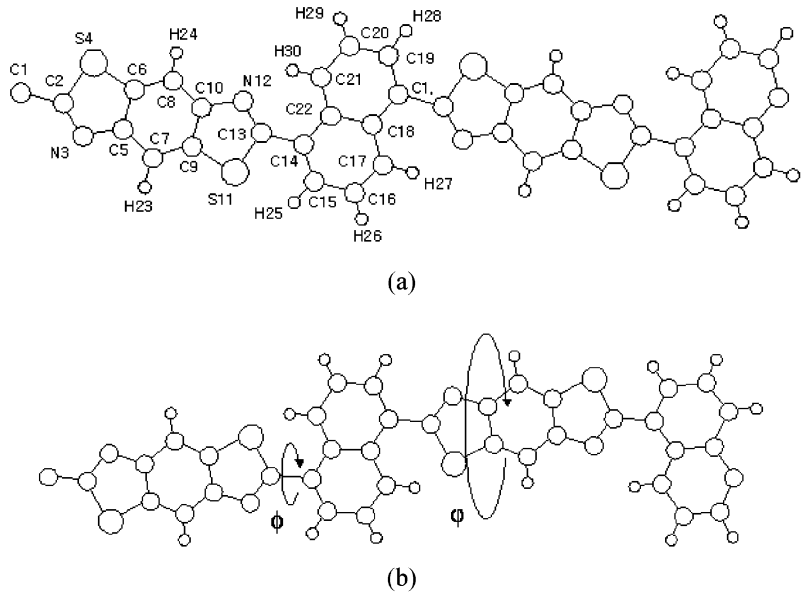

Figure 1. The (a) trans and (b) cis conformations of Naph-1,5-PBT with the numbering of atoms: The torsion angle ϕ is $S_{11}-C_{13}-C_{14}-C_{15}$ and the rotation angle, φ, is 0° when the naphthalene ring is parallel to the *ac* plane in the crystal structure and the clockwise direction is +.

from concentrated HCl in the presence of $SnCl_2 \cdot 2H_2O$. 1,5-Naphthalenedicarboxylic acid was prepared by the hydrolysis of 1,5-naphthalenedinitrile by a mixture of 48% aqueous HBr and glacial acetic acid. It was recrystallized from ethanol prior to use in polymerization.

Synthesis of Poly(benzobisthiazole) Containing Naphthalene-1,5-diyl Unit (Naph-1,5-PBT). Into a resin flask fitted with a high-torque mechanical stirrer, a nitrogen inlet/outlet adapter, and a side opening for addition was placed 2.50 g (0.0116 mol) of 1,5-naphthalenedicarboxylic acid, an equimolar amount of 2,5-diamino-1,4-benzenedithiol dihydrochloride (DABDT, 2.8352 g), and 20.8 g of freshly prepared 77% poly(phosphoric acid) (PPA). The monomers were stirred in PPA, and the resultant mixture was dehydrochlorinated over a period of 24 h under a nitrogen flow, slowly raising the temperature to 105 °C to avoid foaming. The mixture was cooled, and 11.37 g of P_2O_5 was added to "adjust" the PPA composition to have 83% P_2O_5 content[30] and to ensure a final polymer concentration of 10 wt % in PPA. The mixture was maintained at 100 °C with stirring to ensure good homogeneity, the temperature was then raised to 165 °C, and the polymerization was run overnight. During this process, stir opalescence characteristic of the anisotropic phase of the polymer in PPA was observed. The polycondensation was continued at 180 °C for a few hours, and ~30 g of the viscous polymer solution (referred to as the "dope") was taken out for the fiber spinning process. The remaining dope was placed in large quantities of water, and the fibrous polymer was chopped up in a Waring blender. The polymer was filtered off, Soxhlet extracted with hot water, and finally dried in vacuo at 100 °C for 24 h to yield a fibrous, dark yellow solid. The intrinsic viscosity of the polymer, measured in methanesulfonic acid (MSA) at 30 °C, was 13.2 dL/g.

Optical microscopy on the polymer dope was performed using a Leitz polarizing microscope. Thermogravimetric analyses of the bulk polymer were performed in both helium and air using a TA Instruments TGA 2950 analyzer at a heating rate of 10 °C/min.

The polymeric fibers were spun from the lyotropic liquid crystalline phase of the polymer in PPA. Naph-1,5-PBT fibers were fabricated by a dry-jet wet spinning method using a custom-made device. The anisotropic Naph-1,5-PBT/PPA dope (10 wt % polymer) was deaerated at 100 °C and filtered through a 74 μm stainless steel mesh. Naph-1,5-PBT fiber was then spun at 90 °C with a draw ratio of 20. Subsequently, the fiber was soaked in large amounts of distilled water for several days to remove residual solvent. The air-dried fiber was then heat-treated in dry nitrogen at elevated temperatures up to 550 °C for structure development (X-ray diffraction).

For tensile testing, Naph-1,5-PBT fibers were annealed at 350 °C under a nitrogen atmosphere for 10 min. The modulus and the strength were determined using an Instron Universal testing machine at a strain rate of 1%/min.

X-ray Analysis. Wide-angle X-ray diffraction patterns were recorded on a phosphor image plate (Molecular Dynamics) in a Statton camera. Monochromatic Cu Kα radiation from a rotating anode X-ray generator operating at 40 kV and 240 mA was used. The sample to film distance was calibrated by SiO_2 powder. The total intensity of each reflection was measured by using FIT2D software.[31] The intensity of a reflection having a maximum at 2θ (Bragg angle) and ζ (azimuthal angle) was integrated along the azimuthal direction from ζ_1 and ζ_2 at each 2θ, ranging from $2\theta_1$ to $2\theta_2$ ($2\theta_1 < 2\theta < 2\theta_2$ and $\zeta_1 < \zeta < \zeta_2$; $2\theta_1$, $2\theta_2$, ζ_1, and ζ_2 were chosen to include the whole area of the reflection to integrate), then the background was corrected, and finally the peak area was integrated along the 2θ angle. The structure factor was calculated after multiplicity and the Lorenz and polarization correction.[32] The density was measured by flotation in methylene chloride and carbon tetrachloride, which are miscible nonsolvents.

Molecular Modeling. Molecular modeling and simulation of the X-ray patterns were carried out using Cerius2 software. The conformational energy was calculated with the ab initio method using SPARTAN program at the Hatree-Fock 6-31G** level. Figure 1 shows the chemical structure of Naph-1,5-PBT and the numbering of the atoms. Torsion angle ϕ and rotational angle φ are defined as shown in Figure 1. The bond angles and bond lengths were constrained with the values used in the PBT model.[19] The rotational angle φ is defined as the angle between the *ac* plane and the naphthalene ring on the projection along the *c* axis. The conformational energies of the naphthalenebenzobisthiazole-1,5-diyl unit were calculated at 10° increments of the torsion angle ϕ.

Refinement. The structural refinement was performed by using WinLALS software with the constrained least-squares method in which the bond lengths and bond angles were used, as reported by Fratini et al.[19,33,34] The parameters to be refined are the Eulerian angles which are convertible to the rotation angle φ, the torsion angle between the benzobisthiazole and naphthalene ring ϕ, the isotropic temperature factor B_{iso}, and the scale factor.

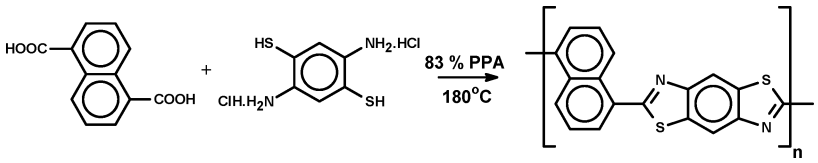

Figure 2. Synthesis of poly(benzobisthiazole) incorporating naphthalene-1,5-diyl unit.

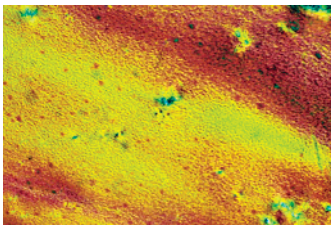

Figure 3. Optical birefringence of 10 wt % Naph-1,5-PBT in PPA, as observed in POM.

Results and Discussion

Polymer Synthesis and Characterization. The reaction scheme for the formation of Naph-1,5-PBT is shown in Figure 2.

Evidence for the presence of the lyotropic mesophase of the rigid-rod polymer in PPA was obtained by the observation of optical birefringence of a sample of the dope sealed between glass slides and examined under polarizing optical microscopy (POM) (Figure 3). The anisotropic texture of the 10% polymer solution in PPA was found to be persistent, even several days after the initial sample preparation.

The polymer was of high molecular weight, as evidenced by its intrinsic viscosity of 13.2 dL/g, measured in a dilute methanesulfonic acid (MSA) solution (initial concentration = 0.10 g/dL) as well as by the fact that the polymer could be continuously spun into fibers from the 10 wt % polymer solution in PPA. Thermogravimetric analysis of the bulk polymer demonstrated the exceptional thermal stability of the polymer, with degradation onset temperatures of 610 and 550 °C respectively in helium and in air.

The measured fiber mechanical properties indicated a tensile modulus of 13.4 GPa and a tensile strength of 0.93 GPa for the as-spun fiber. The heat-treated fibers exhibited an enhancement in mechanical properties, with values of 25.1 and 1.1 GPa respectively for the modulus and the strength. The elongation at break was 7.7% and 5.4% respectively for the as-spun and heat-treated fibers.

In comparison, the typical tensile modulus and strength of heat-treated PBT fibers, spun from 5 to 6 wt % polymer solutions in PPA, have been reported[7] to be 250 and 2.4 GPa, respectively, the measured elongation being 1.5%. Presumably, the rather modest tensile modulus measured for the naph-1,5-PBT fibers relative to that of PBT fibers can be attributed to the kinked structure due to the 1,5-positions of the naphthalene ring at which the polymer chain is extended as well as to the twisted structure due to the large torsion required for the minimum-energy conformation (vide infra for discussion on structural aspects).

Fiber X-ray Pattern. Figure 4a shows the X-ray fiber pattern of Naph-1,5-PBT before annealing. Two broad strong equatorial reflections and several arc-shaped ordered meridional reflections were observed. This pattern is typical of an X-ray fiber pattern of an as-spun rigid-rod polymer. The d-spacings of the two equatorial reflections are ~6.6 and ~3.7 Å. The d-spacing of the second equatorial reflection is similar to that of PBT (3.5 Å), although that of the first equatorial reflection is found to be increased relative to 5.5 Å for PBT. The increase in d-spacing of the first equatorial reflection and the similar d-spacing value for the second one compared to those of PBT suggest that the spacing of the side-by-side packing increases due to the large naphthalene unit, although the spacing due to the face-to-face packing is not significantly affected by the incorporation of a naphthalene unit. The fiber repeat distance along the chain axis is 12.7 Å and is found to be larger compared to that of PBT (12.5 Å). Figure 4b shows the X-ray fiber pattern of Naph-1,5-PBT after annealing. The sharp reflections along the layer lines indicate that a perfect crystal structure was developed during annealing with a high degree of axial orientation in the fiber. This is confirmed by the absence of the streaks along the layer lines which are usually seen in rigid-rod polymers, such as PBT and PBO, implying that Naph-1,5-PBT has a perfect, three-dimensionally oriented crystal structure without axial disorder.

Crystal Structure. Unit Cell Determination. All observed reflections can be indexed by the triclinic cell (metrically monoclinic cell) with parameters of $a = 7.31$ Å, $b = 3.68$ Å, $c = 12.68$ Å, and $\beta = 115.1°$ and the space group of $P\bar{1}$. The calculated density for one monomeric unit in the unit cell is 1.68 g/mL, which is comparable with the measured density of 1.52 ± 0.02 g/mL. Table 1 shows the indices, the observed and calculated d-spacings, and the observed and calculated structure factors (the structure factors will be discussed later). The observed d-spacings are in good agreement with the calculated ones, indicating that the proposed unit cell parameters are accurate. This cell is primitive in contrast to the PBT nonprimitive cell which has two chains in the unit cell. The nonprimitive cell would have twice the a dimension of the unit cell and double the h index of the Bragg indices. All observed reflections, however, can be indexed with the primitive cell, and the model for the cell is accurate enough not to adopt the nonprimitive cell (its model will be discussed later). The three equatorial reflections can be indexed as 100, 010, and 110/200 by the 2-D orthorhombic unit cell with reciprocal lattice parameters of $a^* = 1/6.62$ (1/Å), $b^* = 1/3.68$ (1/Å), and $\gamma^* = 90°$. Figure 5 shows the R and Z values of the observed reflections in the reciprocal cylindrical coordinate. All reflections except for 010 and 011 are located in the two-dimensional a^*c^* reciprocal net. The reflections on the a^*c^* reciprocal net are $h0l$ reflections. The c^* axis is tilted against the meridional direction with the angle between a^* and c^*, β^*, of 65.0°. It is of interest to note that adjacent chains are staggered side-by-side by $c/4$ (c = fiber repeat distance), which is obvious from the same R value of the cylindrical coordinates of the 100 and 004 reflections in Figure 5. Adjacent chains are known to be staggered by $\pm c/4$ for PBO and $\pm c/2$ for PBT in the ac plane, and its + and − directions are random in order to give the disordered structure. The chains, however, are stag-

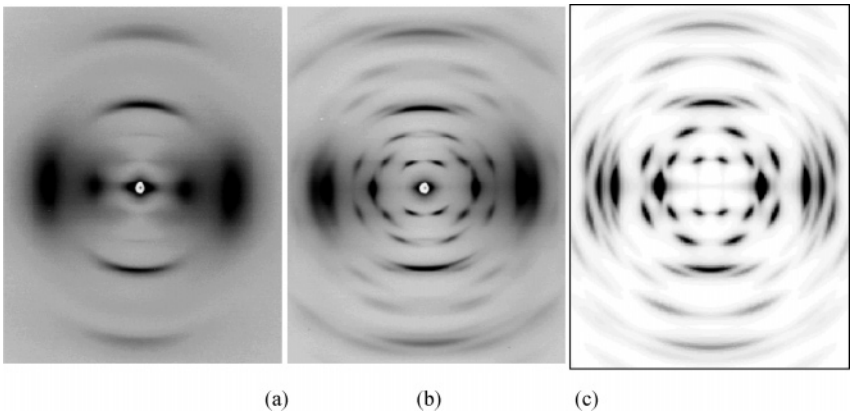

Figure 4. Observed X-ray fiber patterns of Naph-1,5-PBT (a) before and (b) after annealing and (c) the calculated X-ray fiber pattern from the model in Figure 7 in which the crystal sizes were 100 Å in the *a*, *b*, and *c* directions, and fwhm (the full width at half intensity) representing the degree of orientation was 7°.

Table 1. Observed and Calculated *d*-Spacings Based on the Triclinic Unit Cell Parameters of $a = 7.31$ Å, $b = 3.68$ Å, $c = 12.68$ Å, and $\beta = 115.1°$ and the Observed and Calculated Structure Factors Based on the Model in Table 2

h	*k*	*l*	d_o(Å)	d_c(Å)	F_o	F_c
1	0	0	6.62	6.62	69.7	62.9
0	1	0	3.68	3.68	98.3	98.3
2	0	0	3.33	3.31	82.9	89.2
1	1	0		3.21		
0	0	1	11.49	11.49	19.6	10.6
−1	0	1	7.13	7.20	27.8	46.7
1	0	1	4.90	4.91	25.7	18.8
1	1	1	2.87	2.88	21.7	31.4
−1	1	−1				
2	0	1				
−1	0	2	5.78	5.74	24.4	15.7
0	0	2				
−2	0	3	3.26	3.29	32.8	19.5
0	0	3	3.90	3.83	30.4	16.7
−1	1	3	2.84	2.84	16.2	30.7
1	1	−3				
1	0	3				
−2	0	4	2.87	2.87	49.5	33.8
0	0	4				
−1	1	4	2.31	2.30	38.9	30.8
1	1	−4				
1	0	4				
0	0	5	2.30	2.30	38.9	19.4
1	−1	−5	2.08	2.10	19.3	21.5
−1	1	5				
−3	0	5				

gered by *c*/4 with regular direction, i.e., all + (or all −) in the primitive triclinic unit cell of Naph-1,5-PBT.

Chain Conformation. Figure 1 shows the possible trans and cis conformations of Naph-1,5-PBT, which consists of one and two monomeric units, respectively. The fiber repeat distance is identical to the length of one repeat unit, indicating that Naph-1,5-PBT adopts the trans conformation. There are two possible spatial dispositions of the naphthalene ring in the trans conformation; one is for the naphthalene unit being rotated toward nitrogen, and the other is for the naphthalene ring being rotated toward sulfur. Figure 1a is an example of 0°, at which the ring is rotated toward nitrogen. Figure 6 shows the ab initio conformational energy of Naph-1,5-PBT and PBT as a function of the torsion angle, ϕ. The conformational energy of PBT is essentially the same as that reported in the other paper.[35] In the case of PBT, the optimal torsion angle, 0°, is in poor agreement with the X-ray value found for a single crystal of 2,6-diphenylbenzobisthiazole (23.2°),

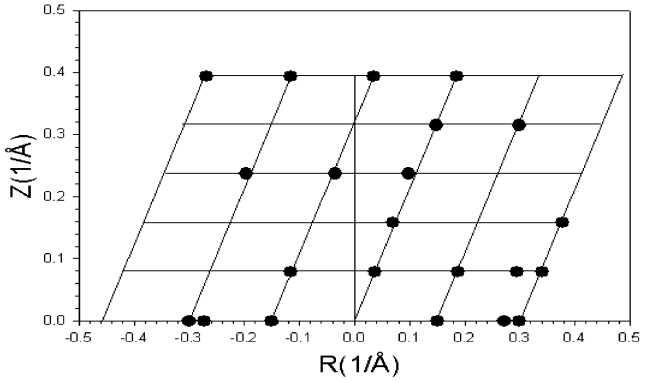

Figure 5. *R* and *Z* values of the observed reflections in the reciprocal cylindrical coordinates. Between the two possible signs of *R* values (+ and − sides), one possible sign was chosen arbitrarily to fit the two-dimensional net.

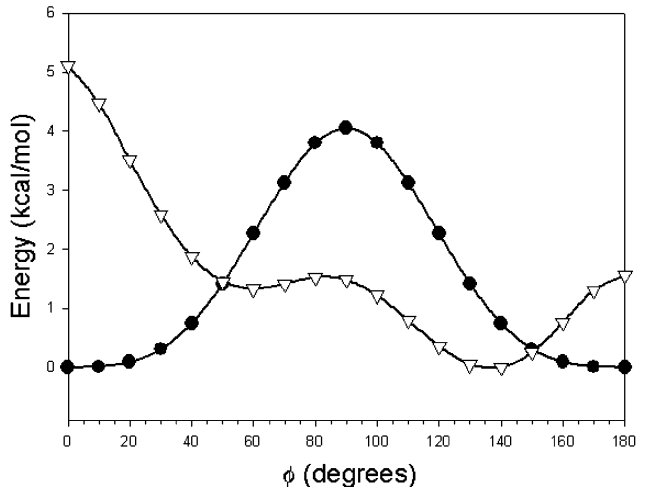

Figure 6. Ab initio conformational energy levels of Naph-1,5-PBT (▽) and PBT (●).

so the discrepancy can be attributed to the crystal packing forces. The energy around the minimum, however, is flat, and the energy difference between the 0° and 30° conformations is 0.39 kcal/mol for PBT. In the case of Naph-1,5-PBT, two energy minima were found at $\phi = \sim 50°$ and $\sim 140°$, with the lower energy minimum occurring at 140°. The conformations at $\phi = \sim 50°$ and $\sim 140°$ are for the naphthalene ring being rotated toward sulfur and nitrogen, respectively. The higher energy at $\phi = 50°$ is presumably due to the steric interaction

Table 2. Final Parameters Obtained by the Constrained LALS Method

parameter		standard deviation
Eulerian angle (deg)		
θ	87.76	
ϕ	142.35	
χ	−1.4	4.6
overall temp factor (Å^2)		
B_{iso}	0.12	
torsion angle		
ϕ (deg)	42	0.27
R-factor (%)		
R	25.46	

Table 3. Fractional Coordinates

atom	x	y	z
C2	−0.0352	−0.0128	0.8936
N3	−0.1767	0.1641	0.8802
C5	−0.1727	0.0956	0.7707
C6	−0.0187	−0.1469	0.6986
S4	0.1206	−0.2848	0.7743
C7	−0.3056	0.2455	0.7300
C9	−0.2810	0.1492	0.6188
C10	−0.1270	−0.0933	0.5467
C8	0.0061	−0.2435	0.5873
S11	−0.4203	0.2871	0.5432
C13	−0.2647	0.0155	0.4240
N12	−0.1231	−0.1616	0.4372
C14	−0.3003	0.0003	0.3173
C15	−0.4930	−0.0205	0.3230
C16	−0.5205	−0.0345	0.2204
C17	−0.3568	−0.0276	0.1134
C18	−0.1648	−0.0069	0.1078
C22	−0.1374	0.0069	0.2097
C1.	0.0000	0.0000	0.0000
C19	0.1923	0.0208	−0.0056
C20	0.2197	0.0346	0.0966
C21	0.0549	0.0277	0.2043
H23	−0.4258	0.4336	0.7844
H24	0.1262	−0.4316	0.5327
H25	−0.6243	−0.0260	0.4088
H26	−0.6738	−0.0510	0.2249
H27	−0.3787	−0.0387	0.0319
H28	0.3236	0.0262	−0.0915
H29	0.3730	0.0512	0.0921
H30	0.0768	0.0388	0.2858

between the large sulfur atom of the heterocyclic ring and α-hydrogen of naphthalene ring. The larger torsion angle, ϕ ($\phi = \sim 140° = -40°$ from 180°), at the minimum-energy level compared to those of PBO (∼0°[21] or 25.7°[22]) and PBT (∼23°) can be attributed to the steric interactions between α-hydrogen and the nitrogen atom, while there is no α-hydrogen causing such steric interactions in PBO and PBT.

Refinement. Table 2 shows the final parameters obtained by the constrained LALS method.[32,33] The $\bar{1}03$ and $\bar{1}05$ reflections, which are near meridian, were omitted in the refinement due to the high Lorenz factor. The refinement converged at $R = 25.46\%$. The comparison between the observed and calculated structure factors is given in Table 1. The final parameters obtained by the constrained least-squares method and the fractional coordinates are given in Table 2 and Table 3, respectively. Regarding the small B_{iso}, 0.12 may be attributed to the rigidity of the molecules.[24] The two parameters, torsional angle ϕ and rotational angle φ, determine chain packing because the unit cell contains one monomeric unit (a single polymer chain). The rotation angle is 4.4 ± 4.6°, which means that the naphthalene ring is nearly parallel to the *ac* plane. The torsion angle, $\phi = 42°$, is the same as the calculated torsion angle from the ab initio method, which means

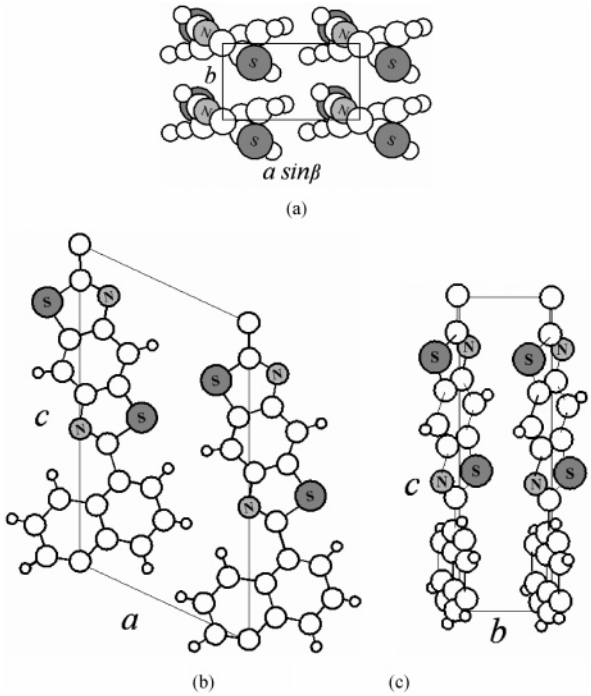

Figure 7. The (a) projection along the chain axis, (b) *ac*, and (c) *bc* projections of the Naph-1,5-PBT model.

that interchain interaction in the crystal does not greatly affect the torsion angle ϕ of the isolated single chain.

Figure 7 shows the projections of the crystal structure. In the projection along the *c* axis (Figure 7a), the chains are packed closely and the naphthalene rings are rotated by 4.4 ± 4.6° from the *ac* plane. In the *ac* projection (Figure 7b), the kinked chains of Naph-1,5-PBT are staggered side-by-side by *c*/4. The *c*/4 staggering between the adjacent chains provides optimum packing in crystal without any steric interaction. In the *bc* projection (Figure 7c), the twisted chains are packed face-to-face without staggering. The large torsion angle ϕ has the least possible chance of slippage of the chains along the *c* direction in the *bc* plane. Naph-1,5-PBT has the kinked structure, which is attributed to the naphthalene unit, as well as the twisted structure, which is introduced by the torsion angle. The kinked and twisted chain structure of the rigid-rod chain in the crystal seems to prevent slippage between the adjacent chains in the crystal structure. The perfect crystal structure of Naph-1,5-PBT may be due to the reduced ease or probability of slippage. Figure 4c shows the calculated X-ray fiber pattern from the model, which is in good agreement with the observed one.

Conclusions

PBT is known to have a lot of axial disorders in the crystal due to the rigidity and the linearity of the chain. Naph-1,5-PBT, synthesized in the current study, has been found to have the kinked structure due to the 1,5-positions of the naphthalene ring at which the heterocyclic rings are extended as well as the twisted structure due to the steric hindrance between the naphthalene and heterocyclic rings. These structural differences change not only the chain conformation but also the crystal structure, especially the axial disorder in the crystal. Naph-1,5-PBT has a perfect three-dimensional crystal structure, unlike rigid-rod polymers such as PBT

and PBO. The crystal structure of Naph-1,5-PBT was investigated using X-ray, molecular modeling methods, and structural refinement. The annealed Naph-1,5-PBT shows the fiber diffraction pattern of a perfect crystal structure, having the triclinic unit cell with parameters of $a = 7.31$ Å, $b = 3.68$ Å, $c = 12.68$ Å, and $\beta = 115.1°$. There is one monomeric unit in the unit cell with the space group of $P\bar{1}$. The measured density was 1.52 ± 0.02 g/mL, which was comparable to the calculated one of 1.68 g/mL. The torsion angle between the heterocyclic and naphthalene rings, ϕ is 138° (= −42° from 180°), at which the naphthalene ring is rotated toward the heterocyclic nitrogen atom; this was derived from the ab initio energy calculation as well as crystal structural refinement. The kinked and twisted structure is well fitted in the crystal. The naphthalene ring is rotated by $4.4 \pm 4.6°$ from the *ac* plane, and the chains are staggered side-by-side by *c*/4 in a regular way in the *ac* plane. Presumably, the kinked and twisted chain structure of the rigid-rod chain in the crystal prevents axial slippage between the adjacent chains in the crystal structure. In other words, the perfect three-dimensional crystal structure of Naph-1,5-PBT might be due to the difficulty in the occurrence of axial slippage in the crystal.

Acknowledgment. This work was supported by a Grant from the Korean Research Foundation (KRF-2002-003-D00091) and the Brain Korea 21 Project. We appreciate Prof. Kenji Okuyama (Tokyo University of Agriculture and Technology) for the fruitful discussions and supplying the winLALS program.

References and Notes

(1) Ulrich, D. R. *Polymer* **1987**, *28*, 533.
(2) So, Y. H. *Prog. Polym. Sci.* **2000**, *25*, 137.
(3) Hu, X. D.; Jenkins, S. E.; Min, B. G.; Polk, M. B.; Kumar, S. *Macromol. Mater. Eng.* **2003**, *288*, 823.
(4) Roche, E. J.; Takahashi, T.; Thomas, E. L. *ACS Symp. Ser.* **1980**, *141*, 303.
(5) Odell, J. A.; Keller, A.; Atkins, E. D. T.; Miles, M. J. *J. Mater. Sci.* **1981**, *116*, 3309.
(6) Adams, W. W.; Eby, R. K. *MRS Bull.* **1987**, *12*, 22.
(7) Allen, S. R.; Filippov, A. G.; Farris, R. J.; Thomas, E. L.; Wong, C. P.; Berry, G. C.; Chenevey, E. C. *Macromolecules* **1981**, *14*, 1135.
(8) Wolfe, J. F.; Arnold, F. E. *Macromolecules* **1981**, *14*, 909.
(9) Wolfe, J. F.; Loo, B. H.; Arnold, F. E. *Macromolecules* **1981**, *14*, 915.
(10) Choe, E. W.; Kim, S. N. *Macromolecules* **1981**, *14*, 920.
(11) Cotts, D. B.; Berry, G. C. *Macromolecules* **1981**, *14*, 930.
(12) Welsh, W. J.; Bhaumik, D.; Mark, J. E. *Macromolecules* **1981**, *14*, 947.
(13) Welsh, W. J.; Bhaumik, D.; Jaffee, H. H.; Mark, J. E. *Polym. Eng. Sci.* **1984**, *24*, 218.
(14) Welsh, W. J.; Mark, J. E. *J. Mater. Sci.* **1983**, *18*, 1119.
(15) Bhaumik, D.; Welsh, W. J.; Jaffee, H. H.; Mark, J. E. *Macromolecules* **1981**, *14*, 951.
(16) Wellman, M. W.; Adams, W. W.; Wolff, R. A.; Dudis, D. S.; Wiff, D. R.; Fratini, A. V. *Macromolecules* **1981**, *14*, 935.
(17) Chu, S. G.; Venkatraman, S.; Berry, G. C.; Einaga, Y. *Marcromolecules* **1981**, *14*, 939.
(18) Wierschke, S. G. Master Thesis, Wright State University, Ohio, 1988.
(19) Fratini, A. V.; Lenhert, P. G.; Resch, T. J.; Adams, W. W. *Mater. Res. Soc. Symp. Proc.* **1989**, *134*, 431.
(20) Martin, D. C.; Thomas, E. L. *Macromolecules* **1991**, *24*, 2450.
(21) Tashiro, K.; Yoshino, J.; Kitagawa, T.; Murase, H.; Yabuki, K. *Macromolecules* **1998**, *31*, 5430.
(22) Takahashi, Y. *Macromolecules* **1999**, *32*, 4010.
(23) Takahashi, Y. *Macromolecules* **2001**, *34*, 2012.
(24) Takahashi, Y.; Sul, H. *J. Polym. Sci., Part B: Polym. Phys.* **2000**, *38*, 376.
(25) Welsh, W. J.; Mark, J. E.; Yang, Y.; Das, G. P. *Mater. Res. Soc. Symp. Proc.* **1989**, *134*, 621.
(26) Yang, Y.; Welsh W. J. *Macromolecules* **1990**, *23*, 2410.
(27) Welsh, W. J.; Yang, Y. *Comput. Polym. Sci.* **1991**, *1*, 139.
(28) Farmer, B. L.; Wierschke, S. G.; Adams, W. W. *Polymer* **1990**, *31*, 1631.
(29) Tonelli, A. E. *Polymer* **2002**, *43*, 637.
(30) Wolfe, J. F. *Encycl. Polym. Sci. Eng.* **1988**, *11*, 601.
(31) www.esrf.fr/computing/scientific/FIT2D/.
(32) Okuyama, K.; Noguchi, K.; Miyazawa, T.; Yui, T.; Ogawa, K. *Macromolecules* **1997**, *30*, 5849.
(33) Arnott, S.; Wonacott, S. *Polymer* **1966**, *7*, 157.
(34) Smith, P. J. C.; Arnott, S. *Acta Crystallogr., Sect. A* **1978**, *34*, 3.
(35) Trohalaki, S.; Dudis, D. S. *Polymer* **1995**, *36*, 911.

MA047967Y